Electron spin resonance study of electron localization and dynamics in metal–molten salt solutions: comparison of M–MX and Ln–LnX_3 melts (M = alkali metal, Ln = rare earth metal, X = halogen)

2003 J. Phys.: Condens. Matter 15 1553

(http://iopscience.iop.org/0953-8984/15/10/304)

INSTITUTE OF PHYSICS PUBLISHING JOURNAL OF PHYSICS: CONDENSED MATTER

J. Phys.: Condens. Matter **15** (2003) 1553–1562 PII: S0953-8984(03)56294-4

Electron spin resonance study of electron localization and dynamics in metal–molten salt solutions: comparison of M–MX and Ln–LnX_3 melts (M = alkali metal, Ln = rare earth metal, X = halogen)

O Terakado, P D Poh[1] and W Freyland[2]

Institute of Physical Chemistry, Physical Chemistry of Condensed Matter Division, University of Karlsruhe, D-76128 Karlsruhe, Germany

E-mail: werner.freyland@chemie.uni-karlsruhe.de

Received 19 November 2002
Published 3 March 2003
Online at stacks.iop.org/JPhysCM/15/1553

Abstract

We have studied the electron spin resonance (ESR) spectra in liquid K–KCl and M–$(NaCl/KCl)_{eut}$ mixtures at different concentrations in salt-rich melts approaching the metal–nonmetal transition region. In both systems F-centre-like characteristics are found. Strongly exchange narrowed signals clearly indicate that fast electron exchange occurs on the picosecond timescale. In contrast, the ESR spectra of a $(NdCl_2)(NdCl_3)$–$(LiCl/KCl)_{eut}$ melt are characterized by a large line width of the order of 10^2 mT which decreases with increasing temperature. In this case, the g-factor and correlation time are consistent with the model of intervalence charge transfer, which is supported by recent conductivity and optical measurements. The different transport mechanisms will be discussed.

1. Introduction

Mixtures of metals and their molten salts can form true solutions over a wide composition range at high temperatures and thus exhibit a continuous transformation from metallic to nonmetallic states (M–NM transition) in a permanent thermal equilibrium [1–3]. In general, a small number of excess electrons released from the metal form localized states, whilst for higher metal concentrations electrons are itinerant. For fluid systems at high temperature the local fluctuation of potential, occurring typically on the order of a picosecond timescale, becomes important and influences the character of the band structure of the system [4]. Electron localization and dynamics in these fluids have been investigated quite intensively in recent years both experimentally [2, 3, 5–7] and theoretically [8–11], especially for alkali metal–alkali metal

[1] Present address: Karl Winnacker Institute, DECHEMA e.V., D-60486 Frankfurt am Main, Germany.
[2] Author to whom any correspondence should be addressed.

0953-8984/03/101553+10$30.00

halide (M–MX) melts because of the relative simplicity of the components. The electronic structure of the salt-rich nonmetallic systems is characterized by strongly localized electronic defect species like F-centres and spin paired dimers or bipolarons. The electronic transport is described by a dynamical equilibrium of localized and mobile electrons where the latter have a constant low mobility of the electrons of the order of 0.1 $cm^2\ V^{-1}\ s^{-1}$ [12].

Within the alkali metal series there is a qualitative difference in the behaviour of the electrical conductivity as a function of composition [13]. In K–KCl melts the equivalent conductivity increases monotonically with addition of metal, reaching the M–NM transition point near a metal mole fraction of $x_K \sim 0.2$ [14], while that of the Na–NaCl system decreases initially [13, 15]. Furthermore, optical absorption spectra of sodium containing melts show a deviation from the so-called Mollwo–Ivey rule, which gives a power law dependence of the optical excitation energy on the ionic radii [3]. Logan [8] proposed that dipolar atomic like states prevail in NaX melts. Xu *et al* [16] carried out quantum molecular dynamics (QMD) simulations of Na–NaBr melts and found a strong tendency to formation of dipolar atomic states of sodium.

In comparison with M–MX melts, the electronic transport properties of polyvalent metal solutions can be different since several stable oxidation states or subhalides can occur. Consequently, electron exchange or intervalence charge transfer (IVCT) between different oxidation states can play an important role in the electronic conduction mechanism of these melts. Examples here are In–InX_3 melts [17] and Ta(IV)–Ta(V) redox systems [18]. Rare earth–rare earth halide (Ln–LnX_3) melts are in this context very interesting systems since the behaviour of electrical conductivity, i.e. the type of electron localization and dynamics, can be rather different within the rare earth series. The conductivity of the lighter rare earth systems (La and Ce) rises steeply with increasing metal concentration, similar to the M–MX melts. On the other hand, that of Nd stays nonmetallic for all concentrations. In addition, the deviation from the linearity of the conductivity between NdI_3 and NdI_2 melts shows a maximum at the concentration of $x_{Nd} \sim 0.17$, which corresponds to the composition of $x_{Nd}^{2+}:x_{Nd}^{3+} = 1{:}1$. From this finding Bredig proposed that the electrical conduction is dominated by electron hopping between divalent and trivalent Nd cations [1]. Recent optical and electrical conductivity measurements indicate that an IVCT mechanism applies in these mixed valent neodymium melts [19, 20].

Electron spin resonance (ESR) is a very useful tool to investigate the nature and dynamics of localized electronic states via the g-factor shift and the resonance line width. This spectroscopic method is, however, very difficult to apply in these melts at elevated temperatures mainly due to their relatively high conductivities and corrosiveness. In a previous ESR study of K–KCl melts up to ~1000 K these problems could be solved [6]. In this paper we present results of ESR measurements for liquid K–KCl and M–$(NaCl/KCl)_{eut}$ (M = Na, K) mixtures at different concentrations in salt-rich melts approaching the M–NM transition region as well as measurements of $LnCl_2$–$LnCl_3$–$(LiCl/KCl)_{eut}$ melts at various temperatures. The experimental techniques are based on previous experiments [6] and will be briefly described in the following section. The results and the main features will be presented in section 3. In section 4.1 the nature of electron localization in M–MX melts is discussed. From the line width data the correlation time of electrons in mixed valent neodymium melts is evaluated and discussed within the model of IVCT in comparison with the recent optical results in section 4.2. The conclusion on the different transport mechanisms is derived in the final section.

2. Experiments

ESR measurements have been carried out using a Bruker EMX X-band spectrometer with a TE_{011} cylinder cavity which combines a 44 W carbon dioxide laser heating system as well

as *in situ* metal doping with coulometric titration method for the measurements of K–KCl and M–$(NaCl/KCl)_{eut}$ melts—for details see [6]. Because of the high liquidus temperatures measurements of binary Na–NaCl melts have not been performed. The advantage of CO_2 laser heating is to avoid the pollution of the cavity e.g. by metal oxides from the standard heating elements, which may lead to a considerable reduction of the cavity quality factor (Q-factor). It should be noted that the electrical conductivities of these melts are rather high, of the order of 1–10 Ω^{-1} cm^{-1}, and the Q-factor is, consequently, rather low. The coulometric titration method allows the precise determination and reproducibility of alkali metal concentration [21, 22]. As an example, for the K–KCl system the electromotive force (EMF) cell consists of

Mo, Ca–Sn(l)|CaF_2(s)|CaF_2, KF–K, K(v), K–KCl(l), Mo (s: solid, l: liquid, v: vapour).

The EMF cell and sapphire ESR cell have been vacuum-tight sealed and an appropriate amount of salt (a few milligrams) was introduced into the sapphire compartment inside an Ar-filled glove box (H_2O, O_2 less than 2 ppm). In order to avoid oxidation of the metal parts and the consequent pollution of the cavity, measurements have been carried out under Ar atmosphere. The amount of metal is controlled *in situ* by variation of the potential applied to the electrochemical cell. For further details of the high temperature set-up see [6].

The ESR parameters are provided by the absorptive part extracted from the mixed absorption–dispersion signal. The spin susceptibility was obtained by comparison of the integrated intensity of the absorptive part of the fitted ESR spectra with the reference sapphire signal which has been calibrated by $CuSO_4{\cdot}5H_2O$ and DPPH (diphenyl picryl hydrazyl) standards at room temperature. The details of spectra analysis are described elsewhere [23].

Because of the extreme corrosiveness of Ln–LnX_3 melts at high temperature against ceramic materials like quartz or sapphire we have carried out ESR measurements of the less corrosive $LnCl_2$–$LnCl_3$–$(LiCl/KCl)_{eut}$ melts employing the high-temperature ESR equipment described above. The appropriate amount of salts has been weighed in a glove box and put into a quartz capillary of 1.5 mm diameter which was sealed under vacuum. The quartz tube with sample was fitted into the sapphire cell which has a better thermal conductivity than quartz, i.e. a homogeneous temperature profile along the quartz cell was achieved. The detailed spectral analysis as has been done for the measurements of M–MX melts was not performed for the ESR spectra of mixed valent rare earth halides because of their rather wide signal, see below.

3. Results

Representative ESR spectra of both M–MX and $LnCl_2$–$LnCl_3$–$(LiCl/KCl)_{eut}$ melts are shown in figure 1. ESR spectra of M–MX melts are characterized by a very narrow signal with a width of the order of 0.1 mT, as depicted in figure 1(A) for M–$(NaCl/KCl)_{eut}$ melts. In contrast, a very wide signal of largest value 110 mT has been observed in the ESR spectra of a $(NdCl_2)_{0.02}(NdCl_3)_{0.02}$–$(LiCl/KCl)_{eut,0.96}$ melt (figure 1(B)). The ESR parameters of this melt are summarized in table 1. From these results we expect a clear difference of the electron localization and dynamics between these melts.

Figure 2 shows the ESR line width of M–MX melts as a function of metal activity as determined from the detailed Lorentz curve analysis of the spectra. In both melts the line width increases monotonically with increasing metal activity. A clearly smaller half width is observed in sodium containing melts, especially prominent at high metal activities. The mole fraction in the K–KCl system is derived from the literature data of the activity as a function of composition and temperature, $a(x, T)$ [22]. Similar data of $a(x, T)$ for the M–$(NaCl/KCl)_{eut}$ system are not known. The present ESR data of the K–KCl system are consistent with the

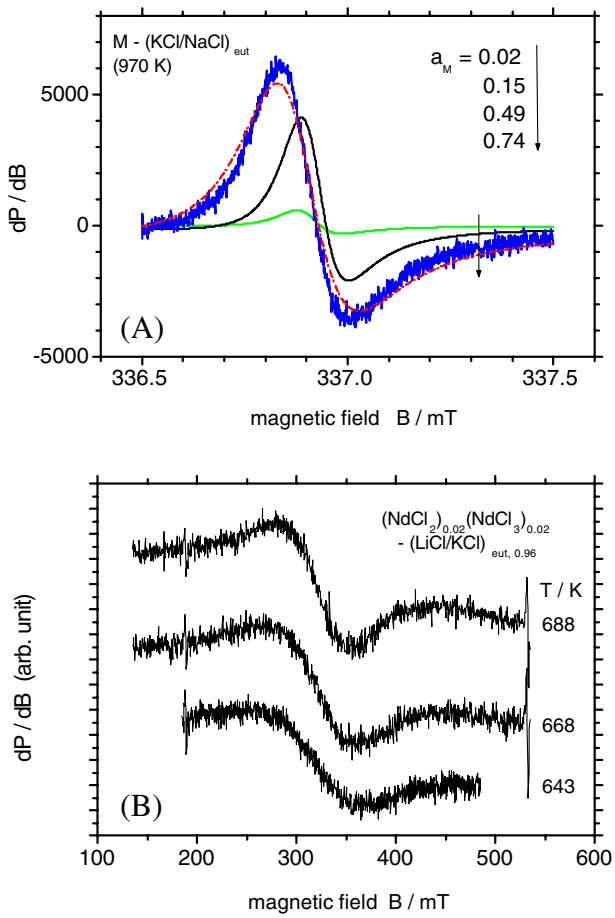

Figure 1. Typical first derivative ESR spectra of molten M–$(NaCl/KCl)_{eut}$ mixtures at 970 K at various metal activities, a_M ((A), upper panel), and of a $(NdCl_2)_{0.02}(NdCl_3)_{0.02}$–$(LiCl/KCl)_{eut,0.96}$ melt at different temperatures ((B), lower panel). The assignments of spectra in the upper panel follow the order of the arrow on the graph. Note that the scales of magnetic field are different for the two graphs. The narrow resonances in B near 185 and 530 mT, respectively, mark the *in situ* measured sapphire signals.

Table 1. Temperature dependence of ESR parameters of a $(NdCl_2)_{0.02}(NdCl_3)_{0.02}$–$(LiCl/KCl)_{eut}$ melt.

T (K)	g-factor	Integrated intensity (arbitrary unit)	ΔB_{pp} (mT)
623	2.11	1.62	110
668	2.10	1.75	93
688	2.08	1.33	78

literature data [6]. Since the corresponding solid state F-centres have a line width of the order of 5–100 mT [24], the strong reduction of half width gives evidence of an exchange narrowing in the liquid state.

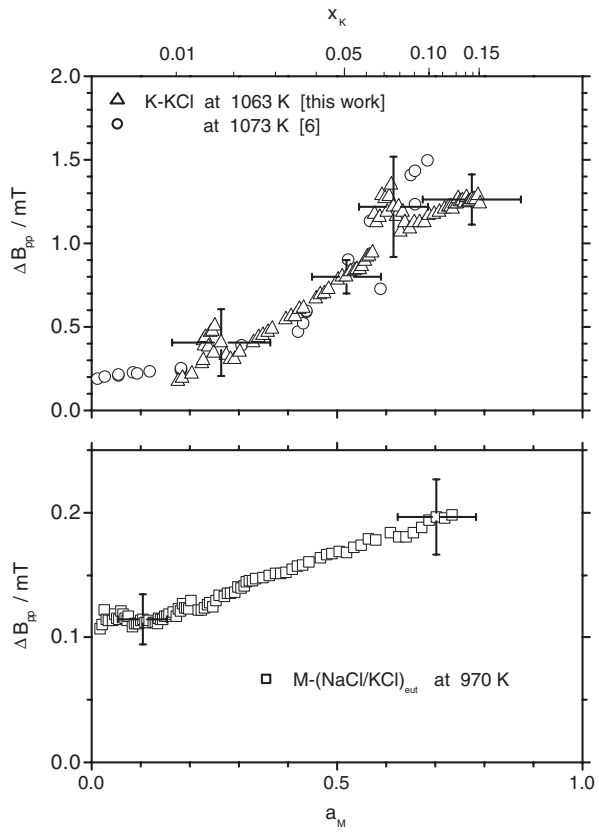

Figure 2. ESR line width as a function of metal activity: comparison of K–KCl at 1063 K and M–$(NaCl/KCl)_{eut}$ melts at 970 K.

The ESR g-factor shift gives information on the nature of localized electronic states. Figure 3 presents the variation of g-factor with metal activity of M–MX melts. In comparison with the previous results [6], the absolute accuracy of the data presented here has been improved by detailed field calibrations [23]. We find a slight systematic difference in the g-factors of the different melts. The g-values observed for liquid K–KCl are lower than those of the corresponding crystalline F-centre at room temperature [24]. This feature of the g-factor shift will be further discussed in the following section.

4. Discussion

4.1. The nature of localized electronic states in M–MX melts

As mentioned in the introductory section, dipolar atomic states have been considered for the Na containing melts [8, 15, 16]. We discuss this problem with respect to the g-factor shift, Δg, of ESR spectra reported here ($\Delta g = g - g_e$ with $g =$ observed g-factor and $g_e = 2.002\,32$ that of the free electron). Assuming that the g-factor shift is dominated by the spin–orbit coupling, it can be approximated by [25]

$$\Delta g \sim -\lambda/\Delta E, \tag{1}$$

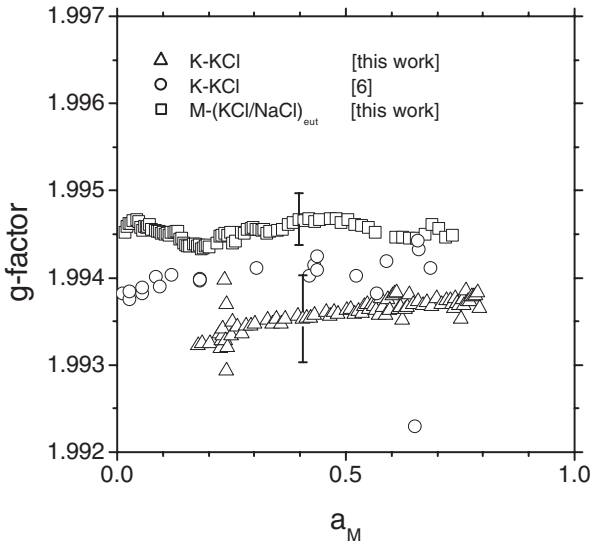

Figure 3. ESR g-factor variation with metal activity of K–KCl in comparison with M–(NaCl/KCl)$_{eut}$, as determined at 1073 and 970 K, respectively, together with the literature data for K–KCl melts [6].

where λ is the spin–orbit coupling constant and ΔE is an electronic excitation energy. In the case of sodium dipolar atomic states, taking the spin–orbit coupling constant of $\lambda_{Na} = 11\ cm^{-1}$ and the transition energy of the sodium D-line ($\lambda = 589$ nm), we have $\Delta g \sim -0.6 \times 10^{-3}$. This shift is considerably smaller than the observed value of the M–(NaCl/KCl)$_{eut}$ melts, i.e. $\Delta g \sim -8 \times 10^{-3}$. More explicit treatment, e.g. considering the hybridization of p orbitals with the ground state, results in an even larger deviation of g-factor shift from the present result [26]. Therefore, the alternative interpretation is that the dominant electronic defect species of Na containing melts are F-centre-like defect species. A quantum chemical consideration yields $\Delta g = -5.3 \times 10^{-3}$ for F-centres in crystalline KCl [27]. Experimental data of the g-factor shift of the crystalline F-centre are known: -4.5×10^{-3} for NaCl and -6.5×10^{-3} for KCl [24]. The greater values in the liquid phase can be explained by a stronger polaronic effect of defect electrons on the cation species. This is measured by the polarizability of cationic species, which is stronger for potassium than for sodium. Here it is interesting that the difference of the g-factor shift between M–(NaCl/KCl)$_{eut}$ and K–KCl melts ($\Delta g \sim -9 \times 10^{-3}$) is around 1×10^{-3}, i.e. half of the g-factor shift difference between F-centres in NaCl and KCl crystals. This is in good agreement with the molar ratio of NaCl and KCl of the eutectic mixture ([NaCl]:[KCl] $\sim$ 1:1). From these considerations the existence of dipolar atomic states in Na containing melts is not consistent with the present ESR data. The electronic defect state is well described by the F-centre-like defect species, analogous to the K–KCl system, so that other defect species like bipolarons should be responsible for the peculiarities in the physical properties of the Na containing melts, e.g. their deviation from the Mollwo–Ivey law or initial conductivity behaviour [3, 13, 15].

Figure 4 shows the number density of paramagnetic species of M–MX melts evaluated from the spin susceptibility, whereby the paramagnetic species are assumed to follow the Curie law. Also plotted is the number density assuming that all metal atoms release one excess electron with Curie paramagnetism. The values of both K–KCl and M–(NaCl/KCl)$_{eut}$ melts

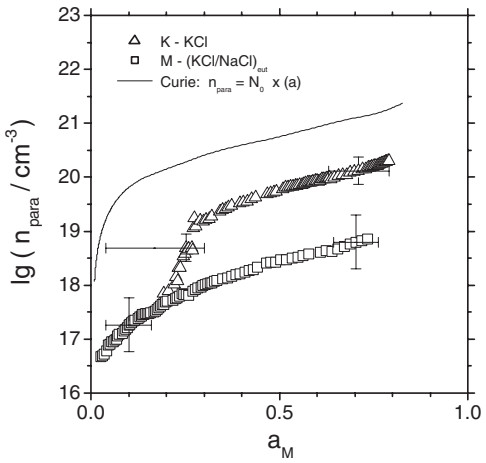

Figure 4. Number density of paramagnetic species of K–KCl and M–$(NaCl/KCl)_{eut}$ melts plotted logarithmically versus metal activity. Included in the figure is the number density of spins (curve), whereby each metal atom is assumed to release an electron obeying the Curie law.

are smaller than that of purely Curie susceptibility, clearly indicating that spin pairing occurs in these systems at low metal concentrations. Especially, the Na containing melts exhibit a lower spin density, i.e. stronger tendency for the formation of bipolaronic electronic defect species in comparison with K–KCl melts. Xu *et al* [16] found in their QMD simulations that besides dipolar atomic states other defect species like paramagnetic F-centres or molecular-like structures, e.g. Na_2^+, could form in Na–NaBr melts. Furthermore, the formation of spin paired states like Na^- or bipolaronic complexes is considered. The mobility of spin paired species is low [10], which explains the reduction of electrical transport and the consequent decrease of the equivalent conductivity in the sodium system, as first pointed out by Bredig [1] and Warren *et al* [15].

As for the electron dynamics in the present systems, the very narrow signal of the ESR half width indicates strongly that the signal is dominated by motional narrowing. The NMR relaxation time of salt-rich solutions of Cs–CsI melts is of the order of $\tau_c \sim 10^{-12}$ s [2]. Assuming that the contribution from the surface relaxation due to the skin effect [28] and the line broadening due to magnetic field inhomogenities can be neglected, the exchange narrowed line width, ΔB_{exch}, can be approximated for the Lorentzian ESR line shape by

$$\Delta B_{\text{exch}} = \sqrt{3}\gamma B_O^2 \tau_c, \tag{2}$$

where γ is the gyromagnetic ratio and B_O is here the line width of the crystalline F-centre. Taking the value of $B_O = 4$ mT for crystalline F-centres in KCl [24] and the above correlation time, we obtain an exchange narrowed line width of about 10^{-1} mT, which is of comparable magnitude with present data, i.e. $\sim 10^{-1}$ mT. This consideration indicates that the ESR signal is due to the average contribution of F-centre-like and mobile electrons, whereby a fast dynamic equilibrium occurs between these two species [6]. The difference in line width of the K–KCl and M–$(NaCl/KCl)_{eut}$ systems implies that in the latter system the upper limit for the number of paramagnetic species is reached very fast, so that the line width shows only a subtle increase with metal activity.

4.2. Electron localization and dynamics in $(NdCl_2)_{0.02}(NdCl_3)_{0.02}$–$(LiCl/KCl)_{eut,0.96}$

Rare earth metal ions are characterized by strong spin–orbit coupling (600–3000 cm^{-1}) which leads to a strong coupling of the spins to the lattice and very small spin relaxation times [25]. As a consequence the ESR lines are extremely broadened and typically can only be detected at very low temperatures, though this is not the case for a system with S configuration of spin system, e.g. Gd^{3+} where ESR signals are observed at room temperature [29].

The ESR spectra observed here for the mixed valent neodymium chloride melts at elevated temperatures have a band width of the order of 10^2 mT which is reduced with increasing temperature. This is indicative of exchange or motional narrowing of the resonances, and the interesting question is what the magnitude of the electronic correlation time τ_e is and how it compares with the corresponding estimate from the optical spectra and electronic conductivities. With this aim the microcrystalline model of McConnell is used [30] where the metal ions with spin 1/2 and their ligands are treated as an octahedral unit in solution. Based on the Raman data of LnX_3–MX melts [31] the assumption of octahedral species should be allowed for the present systems with dilute rare earth halide concentrations. Within the model and with the assumption of exchange narrowing, i.e. $\omega\tau_e \ll 1$, the ESR line width at half maximum, $\Delta\omega_{1/2}$, is determined by the transverse relaxation rate, $1/T_2$, which is given by [29]

$$\Delta\omega_{1/2} \approx \frac{1}{T_2} \approx \frac{8\pi^2(\Delta g g \mu_B B_0 + \Delta A I_z)\tau_e}{15h^2}, \tag{3}$$

where $g = (1/3)g_\parallel + (2/3)g_\perp$, $\Delta g = g_\parallel - g_\perp$ and $\Delta A = A_\parallel - A_\perp$ with g = g-factor, A = hyperfine coupling constant, ω_0 = resonance frequency, μ_B = Bohr magneton, h = Planck constant, I_z = z-component of nuclear spin and the subscripts, $\parallel$ and $\perp$, mean, respectively, the component parallel (z-direction) and vertical to the static magnetic field, B_0. The values of Δg and ΔA can only be estimated from ESR data for Nd^{3+} ion in a $LaCl_3$ crystal at 4 K, see e.g. [29]. This results in a value of $\tau_e \sim 10^{-12}$ s.

We have recently presented the optical spectra of NdI_2–NdI_3 melts and the excitation around 1.6 eV is interpreted as the IVCT band, whereby the system is described by a simple one-electron two-(cation-)site model [20]. From this result we calculate the electron transfer rate, W, according to [32]:

$$W = \frac{2\pi}{h} J^2 \left(\frac{\pi}{4k_B T E_A}\right)^{1/2} \exp\left(-\frac{E_A}{k_B T}\right). \tag{4}$$

Here E_A is thermal activation energy and J is the resonance integral or coupling constant, which is given from the Hush–Marcus theory [33] by

$$J = \frac{2.05 \times 10^{-2}\sqrt{\tilde{\nu}\Delta\tilde{\nu}_{1/2}\varepsilon_{\max}}}{R_{MM}}, \tag{5}$$

where J is given in cm^{-1}, $\tilde{\nu}$ is the wavenumber at the maximum of the IVCT band, $\varepsilon_{\max}$ is its molar absorptivity, $\Delta\tilde{\nu}_{1/2}$ is the width at half maximum of the polaron band in cm^{-1} and R_{MM} is the distance between two metal sites in ångstrom. Taking R_{MM} as 3 Å, we obtain a value of $W \sim 10^{12}$ s^{-1} at 800 °C. This result of W^{-1} is comparable with the relaxation time τ_e from ESR estimated above.

This discussion of the results of the ESR measurements, together with the recent electrical conductivity and optical measurements, supports the interpretation of the experimental data by IVCT between di- and trivalent rare earth ions occurring in mixed valent neodymium melts. A simple two-site model can reasonably well describe the electronic transport properties of these melts. These characteristics of IVCT were first reported for crystalline mixed valence systems like europium [34] and ytterbium chlorides [35].

5. Conclusion

The ESR spectra in liquid K–KCl and M–$(NaCl/KCl)_{eut}$ mixtures at different concentrations in salt-rich melts approaching the metal–nonmetal transition region presented here reveal F-centre characteristics in both systems. The existence of dipolar atomic defect species, as anticipated in QMD calculations [16], is not supported by the present ESR data in a Na containing melt. The peculiarities of Na containing melts concerning e.g. equivalent conductivities or deviation from the Mollwo–Ivey law are rather explained by the stronger formation of spin paired or bipolaron species. Strongly exchange narrowed signals in both M–MX melts clearly indicate that the electron dynamics occurs on the picosecond timescale. The ESR spectra of a $(NdCl_2)(NdCl_3)$–$(LiCl/KCl)_{eut}$ melt are characterized by a large line width of the order of 10^2 mT which decreases with increasing temperature. The g-factor and correlation time are consistent with the model of IVCT, which is supported by recent conductivity and optical measurements.

Acknowledgments

We acknowledge financial support by DFG through SFB 195 and partly by Fonds der Chemischen Industrie.

References

[1] Bredig M A 1964 *Molten Salt Chemistry* ed M Blander (New York: Interscience) p 367
[2] Warren W W Jr 1987 *Molten Salt Chemistry (NATO ASI Series No 202)* ed G Mamantov and R Marassi (Dordrecht: Reidel) p 237
[3] Freyland W 1995 *Metal Nonmetal Transitions Revisited* ed P Edwards and C N R Rao (London: Taylor and Francis) p 167
[4] Logan D E and Siringo F 1992 *J. Phys.: Condens. Matter* **4** 3695
[5] Nattland D, Blanckenhagen B v, Juchem R, Schelkes E and Freyland W 1996 *J. Phys.: Condens. Matter* **6** 9309
[6] Schindelbeck T and Freyland W 1996 *J. Chem. Phys.* **105** 4448
[7] Blanckenhagen B v, Nattland D, Bala K and Freyland W 1999 *J. Chem. Phys.* **110** 2652
[8] Logan D E 1986 *Phys. Rev. Lett.* **57** 782
Logan D E 1987 *J. Chem. Phys.* **86** 234
[9] Selloni A, Carnevali P, Car R and Parrinello M 1987 *Phys. Rev. Lett.* **59** 823
[10] Fois E S, Selloni A, Parrinello M and Car R 1988 *J. Phys. Chem.* **92** 3268
[11] Koslowski T 1997 *J. Chem. Phys.* **106** 7241
[12] Haarberg G M, Osen K S, Egan J J, Heyer H and Freyland W 1988 *Ber. Bunsenges. Phys. Chem.* **92** 139
[13] Bronstein H R and Bredig M A 1958 *J. Am. Chem. Soc.* **80** 2077
[14] Nattland D, Heyer H and Freyland W 1986 *Z. Phys.* **149** 1
[15] Warren W W Jr, Sotier S and Brennert G F 1983 *Phys. Rev. Lett.* **50** 1505
[16] Xu L F, Selloni A and Parrinello M 1989 *Chem. Phys. Lett.* **162** 27
[17] Ichikawa K and Warren W W Jr 1979 *Phys. Rev.* B **20** 900
Warren W W Jr, Schönherr G and Hensel F 1983 *Chem. Phys. Lett.* **96** 505
[18] Stöhr U and Freyland W 1999 *Phys. Chem. Chem. Phys.* **1** 4383
[19] Terakado O, Zein El Abedin S, Endres F, Nattland D and Freyland W 2002 *J. Non-Cryst. Solids* **312–314** 459
[20] Zein El Abedin S, Terakado O, Endres F, Nattland D and Freyland W 2002 *Phys. Chem. Chem. Phys.* **4** 5335
[21] Egan J J 1985 *High Temp. Sci.* **19** 111
[22] Bernard J, Blessing J, Schummer J and Freyland W 1993 *Ber. Bunsenges. Phys. Chem.* **97** 177
[23] Poh P D 2001 *PhD Thesis* University of Karlsruhe
available on the internet at http://www.ubka.uni-karlsruhe.de/eva/
[24] Seidel H and Wolf H C 1968 *Physics of Color Centers* ed W B Fowler (New York: Academic) p 537
[25] Carrington A and McLachlan A D 1967 *Introduction to Magnetic Resonance* (New York: Harper and Row)
[26] Kahn A H and Kittel C 1953 *Phys. Rev.* **89** 315
[27] Gourary B S and Adrian F J 1960 *Solid State Phys.* **10** 127

[28] Dyson F J 1955 *Phys. Rev.* **98** 349
[29] Ayscough P B 1967 *Electron Spin Resonance in Chemistry* (London: Methuen)
[30] McConnell H M 1956 *J. Chem. Phys.* **25** 709
[31] Photiadis G M, Borresen B and Papatheodorou G N 1998 *J. Chem. Soc. Faraday Trans.* **94** 2605
[32] Böttger H and Bryksin V V 1985 *Hopping Conduction in Solids* (Weinheim: VCH)
[33] Hush N S 1967 *Prog. Inorg. Chem.* **8** 391
Hush N S 1985 *Coord. Chem. Rev.* **64** 135
[34] Lange F T 1992 *PhD Thesis* University of Karlsruhe
[35] Haselhorst R W 1994 *PhD Thesis* University of Karlsruhe